

## The effect of washing on stabilized and unstabilized low-density polyethylene films naturally weathered in a sub-Saharan region (Ghardaïa, Algeria)

Souad BEHISSA , Salem Fouad CHABIRA , Nourelhouda BENMILOUD\* ,  
Mohamed SEBAA 

Department of Engineering Processes, Mechanics Laboratory (Lme)-RFME, Faculty of Technology,  
Amar Telidji University, Laghouat, Algeria

Received: 27.10.2018

Accepted/Published Online: 07.01.2019

Final Version: 03.04.2019

**Abstract:** The effect of washing stabilized and unstabilized blown extruded films of low-density polyethylene (LDPE) used for greenhouse coverings naturally weathered in a sub-Saharan facility at Ghardaïa (Algeria) for 19 and 6 months, respectively, was studied. A comparison between unwashed and daily washed samples was done. The changes in the films' properties were followed at regular intervals using various characterization methods (physicochemical and mechanical). Although in both cases the chemical species formed due to the weathering were qualitatively the same, they essentially differed in their concentrations, namely they were higher for the washed samples than for the unwashed ones. Inversely, the crystallinity of the washed samples was lower. Contrary to expectations, the decrease in the tensile strength and elongation at break was delayed as a result of the washing, despite a higher oxidation rate.

**Key words:** Low-density polyethylene, films, aging, washing, properties, characterization, greenhouse coverings

### 1. Introduction

Polyethylene is the most widespread polymer in the world and global demand was expected to reach 99.6 million tons in 2018. One of the most popular applications of polyethylene is in the agricultural field as films for greenhouse coverings. Low-density polyethylene (LDPE) films have progressively replaced glass as coverings because of their low cost, lightness, and resistance to moisture and chemical agents. However, outdoor exposure of PE films results in photolytic, thermal, and photooxidative degradation, all associated with chemical changes. The interaction with surrounding oxygen causes an initial formation of hydroperoxides,<sup>1,2</sup> with decomposition of the transient hydroperoxide intermediates giving rise to many oxygenated products (aldehydes, carboxylic acids, ketones, etc.), whose relative amounts vary as a function of exposure time. In parallel with the oxidation, the formation of unsaturated structures, such as vinyl and trans-vinylenes, and the disappearance of others, such as vinylidenes, occurs. Tidjani et al.,<sup>3</sup> Chabira et al.,<sup>4</sup> and Salvalaggio et al.<sup>5</sup> showed the molecules alterations were mainly governed by crosslinking and chain scission reactions by Fourier transform infrared spectroscopy analysis. Moreover, Salvalaggio et al. showed that carboxylic acids were the prevailing carbonyl species in terms of formation.<sup>5</sup> Unlike these results, Yagoubi et al.<sup>6</sup> found that aldehydes were the predominant carbonyl species. In general, the growth of these oxidized species leads to a drastic loss of the mechanical performance of the material by reducing its ductility (i.e. ultimate properties) and increasing its stiffness (Young's modulus).<sup>4,7</sup>

\*Correspondence: nh.benmiloud@lagh-univ.dz

Therefore, quantitative determination of these species and following of their growth are needed to give a better insight into the oxidation mechanism.

On the other hand, the production of stabilized grades of LDPE, with numerous photostabilizing additives such as ultraviolet absorbers (UVAs) and hindered amine light stabilizers (HALSs), has partially answered consumer demand because these stabilizers can produce a significant improvement in the lifetime of the LDPE, i.e. a delay in the deterioration of mechanical properties. HALSs have proved to be very effective in inhibiting photooxidation, especially with polyolefins.<sup>8,9</sup> During their investigation, Sebaa et al. found that stabilized LDPE films were much more resistant to environmental stresses during weathering compared to an unstabilized grade, giving them a longer service lifetime.<sup>10</sup> The effect of stabilization on the photodegradation behavior of LDPE films has also been studied by Fehine et al.<sup>11</sup> They found that samples stabilized with a UV absorber were less affected in terms of their tensile properties due to a lower reduction in molecular sizes, compared to unstabilized samples, which displayed a considerable drop.

However, despite the addition of stabilizers enhancing material performance and endurance, material deterioration after a season cycle or two is not prevented. This remains a major inconvenience from both the practical and economic points of view. Many research works have dealt with the effect of outdoor exposure on modifications of the structural and mechanical properties of both stabilized and unstabilized films, but we know of none that has considered the effect of film maintenance by washing.

In the present work two grades of LDPE films were investigated, a stabilized (S) and an unstabilized grade (U). Both films were naturally weathered in a sub-Saharan facility. Four protocols were conducted; for two of them the stabilized and unstabilized films were washed, while for the other two they were unwashed. To follow the microstructural and mechanical changes undergone by the films, various characterization methods were used (Fourier transform infrared-attenuated total reflectance spectroscopy (FTIR-ATR), differential scanning calorimetry (DSC), and tensile testing). The analysis of the results not only showed the effect of aging but also that of washing on the greenhouse covering films during their service.

## 2. Results and discussion

### 2.1. Solar energy

The solar energy (E) was measured daily at three different periods of the day (0800, 1300, and 1700 hours) for the duration of the aging protocols for both the unstabilized and stabilized films. The solar energy variation (Figure 1) shows the expected results since it reached a maximum in the middle of the day with intense insolation, and was medium at the beginning (0800 hours) and the end (1700 hours) of the day due to weak sunshine near the sunrise and sunset corresponding to the lower angle of incidence of the low sun's rays.

### 2.2. FTIR analysis

The infrared spectra of the unaged stabilized and unstabilized films are shown in Figure 2. The spectra show the presence of a wide band with a maximum frequency at  $2910\text{ cm}^{-1}$  corresponding to the stretching vibration of the symmetric C-H bonds of the methylene  $\text{CH}_2$  group.<sup>12</sup> The broad absorption band showed maxima at  $1472$  and  $1463\text{ cm}^{-1}$  attributed to the bending deformations of the methylene  $\text{CH}_2$  groups in the crystalline and amorphous phases, respectively.<sup>13</sup>

These two phases also showed separated peaks due to rocking deformation of the methylene ( $\text{CH}_2$ ) groups, appearing as a doublet at  $729$  and  $721\text{ cm}^{-1}$ .<sup>14</sup> The broad absorption band going from  $1200$  to  $885\text{ cm}^{-1}$ ,

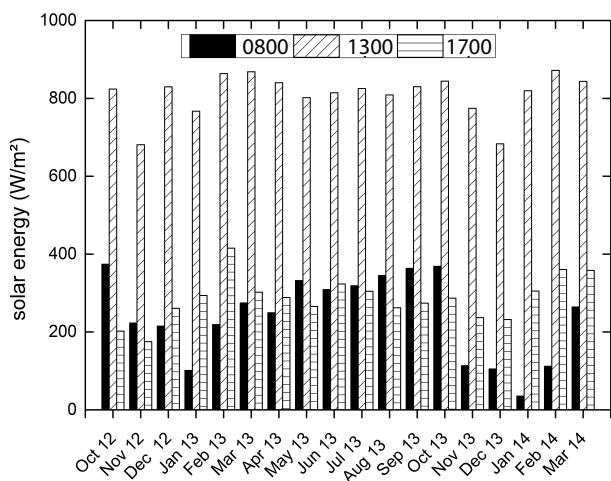


**Figure 1.** Monthly average solar energy of different periods of the day (0800, 1300, and 1700 hours).

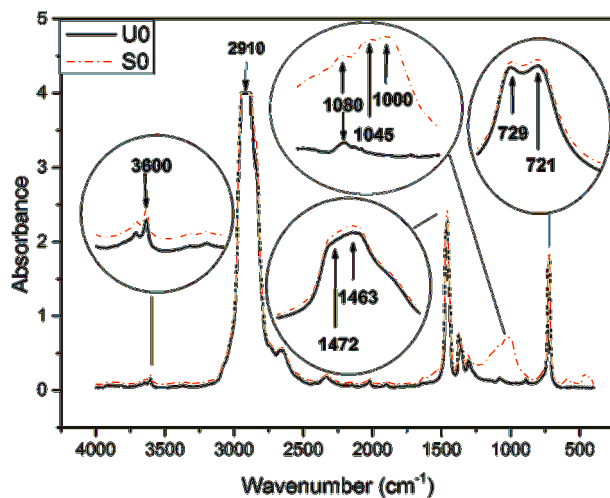


**Figure 2.** Infrared spectra of unaged films (unstabilized and stabilized).

particularly well developed for the stabilized grade, was resolved into a large peak at  $1000\text{ cm}^{-1}$  with two other maxima, at  $1045$  and  $1080\text{ cm}^{-1}$ , which are attributed to the stretching vibrations of C–O bonds belonging to the alcohols  $\text{RCH}_2\text{–OH}$  for the first and to ether  $\text{R–O–R}$  groups for the last two peaks.<sup>15</sup>

The same types of data for the naturally weathered stabilized and unstabilized and unwashed and washed samples are shown in Figures 3 and 4, respectively. A cursory observation of the FTIR spectra of both the stabilized (Figures 3a and 3b) and unstabilized (Figures 4a and 4b) grades aged under natural weathering shows that the washing cycle did not result in any particular differences between them.

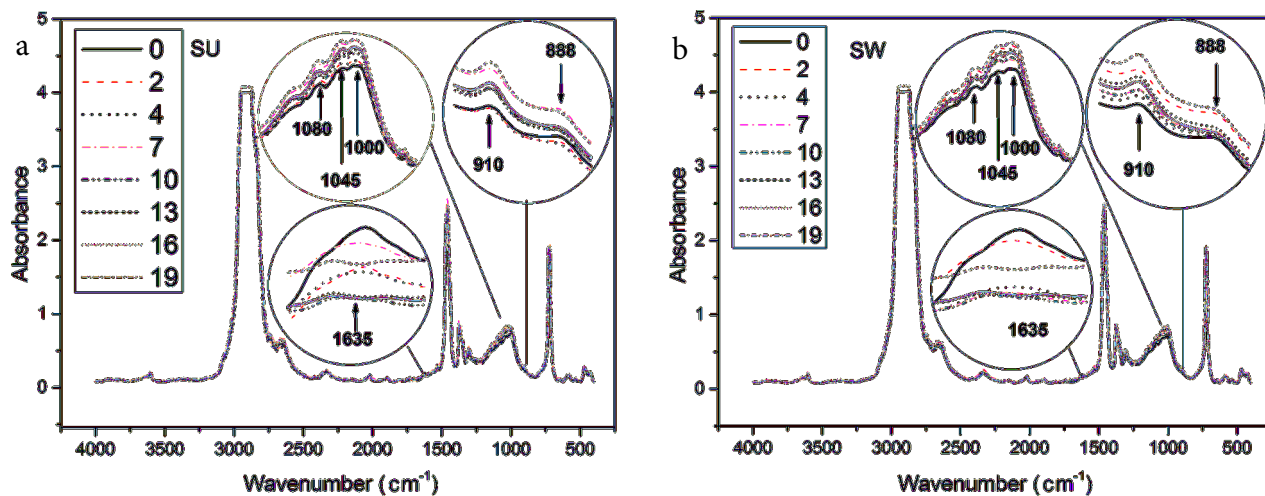


**Figure 3.** Infrared spectra of naturally weathered stabilized samples for 0 to 19 months' exposure: a) unwashed, b) washed.

For the stabilized LDPE samples (Figures 3a and 3b) we observe the following:

- Two peaks with very weak intensity, one at  $888\text{ cm}^{-1}$ , assigned to vinylidene groups ( $>\text{C}=\text{CH}_2$ ), and the other at  $910\text{ cm}^{-1}$ , corresponding to the vinyl groups ( $\text{R}_2\text{C}=\text{CHR}$ ), having also a stretching vibration

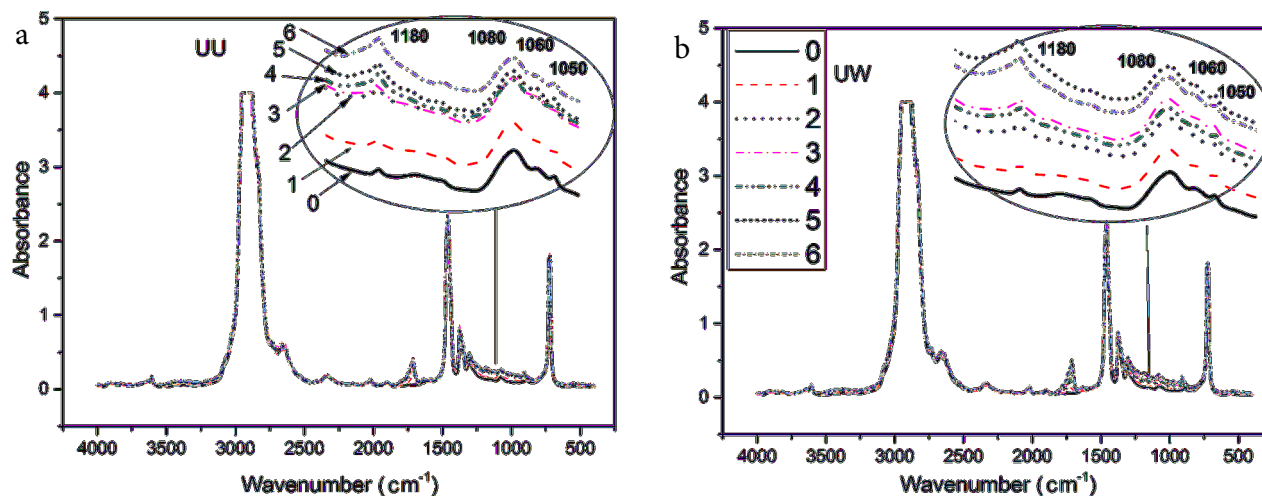


Figure 4. Infrared spectra of naturally weathered unstabilized samples: a) unwashed, b) washed.

in the composite band centered at  $1635\text{ cm}^{-1}$ ; this band encompasses many other vibrations belonging to other groups.<sup>10,16–18</sup> This region of unsaturations ( $880\text{--}920\text{ cm}^{-1}$ ) changed with aging; the peak of vinylidenes ( $888\text{ cm}^{-1}$ ) decreased, while that of vinyls ( $910\text{ cm}^{-1}$ ) increased.

- A slightly increasing, intense, massive band, situated in the range  $1200\text{--}925\text{ cm}^{-1}$ , which encompasses the stretching vibrations of the C–O belonging to alcohols and ethers.

For the unstabilized LDPE samples (Figures 4a and 4b) we observe the following:

- Two peaks developed progressively: one at  $1080\text{ cm}^{-1}$ , with shoulders at  $1060$  and  $1050\text{ cm}^{-1}$ , and the other at  $1180\text{ cm}^{-1}$ , attributed to the stretching vibrations of C–O bonds belonging to ether ( $1080\text{--}1050\text{ cm}^{-1}$ ) and aliphatic ester ( $1180\text{ cm}^{-1}$ ) groups, respectively.<sup>15,19</sup> Ethers very probably formed during polymerization in the radical process (trapped oxygen in the chain, resulting in manufacturing defects). The formation of esters justifies the photooxidation mechanism.<sup>3</sup>
- In enlargements of parts of the two spectra (Figure 5) we observe two growing peaks at  $990$  and  $909\text{ cm}^{-1}$ , both corresponding to the C=C vibration of vinyl ( $\text{RCH}=\text{CH}_2$ ) groups (Figure 5a). These unsaturations were also visible at  $1640\text{ cm}^{-1}$  (Figure 5b). Another peak, at  $966\text{ cm}^{-1}$  in Figure 5a, belongs to the trans-vinylene groups ( $\text{RHC}=\text{CRH}$ ). The peak at  $888\text{ cm}^{-1}$ , attributed to vinylidene  $>\text{C}=\text{CH}_2$  groups, disappeared progressively with increased aging.<sup>10,16–18</sup>
- The progressive increase in the absorption band with peaks at  $1712\text{ cm}^{-1}$ , with shoulders on its left side (Figure 5b), is attributed to C=O stretching of many carbonyl species (acids, ketones, ketoacids, aldehydes, lactones, esters etc.). Esters presented additional stretching vibrations of the C–O bond at  $1180\text{ cm}^{-1}$  (Figure 4).<sup>5,20</sup> The peaks situated at  $1712\text{ cm}^{-1}$ ,  $1730\text{ cm}^{-1}$ , and  $1781\text{ cm}^{-1}$  belong to H-bonded carboxylic acids, aldehydes, and  $\gamma$ -lactones, respectively.<sup>21,22</sup>

In addition to the carbonyl products recognizable by shoulders at  $1730$  and  $1781\text{ cm}^{-1}$ , this complex absorption band ( $1800\text{--}1680\text{ cm}^{-1}$ ) also encompasses a variety of hidden carbonyl products. An overall curve-

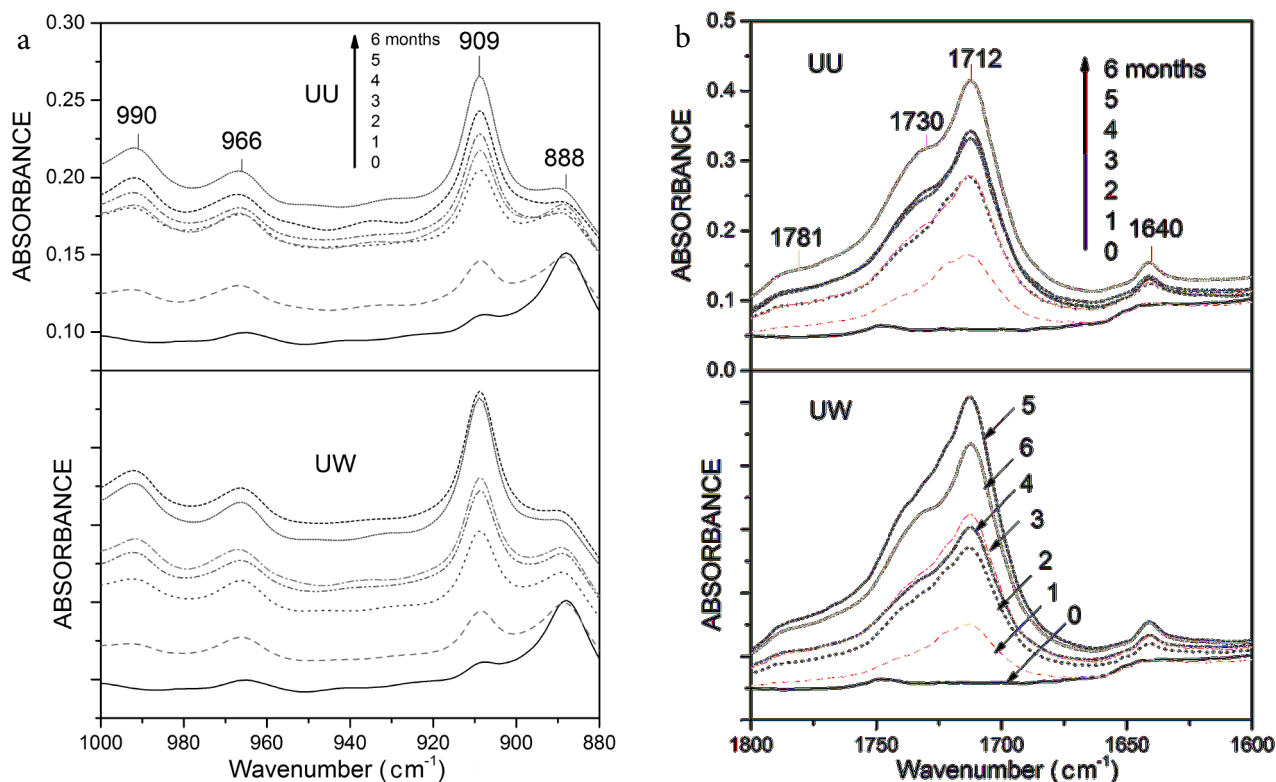


**Figure 5.** Infrared absorbance spectra recorded from the unstabilized LDPE 2100 T N00W films for various aging stages (0, 2, 4, and 6 months): a) unsaturation stretching region (vinylidene, vinyl, and trans-vinylene), b) carbonyl stretching region.

fitting analysis, collected and given as supplementary material in this paper (see Figure S1), highlights not only the hidden and the overlapped absorption bands, but also their intensities. The data obtained from the spectra deconvolution for the different aging stages showed an increasing oxidation level and the mathematical decomposition of the band envelope revealed a growing component number constituting the complex absorption band. However, for the unexposed sample (Figure S1a) a good fitting reveals the contribution of 4 components constituting the overall envelope. With aging the number of components can rise to 13 (Table 1). Most of them have already been mentioned by Salvalaggio et al.<sup>5</sup>

A comparison of the carbonyl envelope of 6-month-aged weathered UW and UU samples show that the deconvoluted peaks of the washed samples were slightly higher in intensities except for the peak at  $1728\text{ cm}^{-1}$  (Figures S1b and S1c).

The change in the carbonyl species concentration with aging time of the naturally weathered UU and UW LDPE films, calculated by curve-fitting analysis of the IR spectra, is shown in Table 2. The concentration of aldehydes was obtained by subtracting the concentration of esters, which was determined from the band situated at  $1180\text{ cm}^{-1}$ , from the composite peak situated at  $1737\text{ cm}^{-1}$ , which was assigned to aldehydes and esters (Table 1). The same mathematical method was applied by Salvalaggio et al.<sup>5</sup> For both UU and UW LDPE films, the formation of the carbonyl species was dominated by aldehydes followed by acids (isolated and associated), ketones (terminal and in-the-chain), ketoacids, lactones, and esters. It appears that the formation of the last two products was not favored and their concentrations were almost negligible. Salvalaggio et al. and

**Table 1.** Assignment of the component bands in the carbonyl region of the infrared spectrum.

Component no.	Peak position (cm <sup>-1</sup> )	Assignment	Aging (months)		Washing
			0	6	
1	1687	Ketones, acids $\alpha, \beta$ unsaturated	-	+	Unwashed
			-	+	Washed
2	1699	$\gamma$ -Ketoacids, keto group	-	+	Unwashed
			-	+	Washed
3	1712	H-bonded carboxylic acids	-	+	Unwashed
			-	+	Washed
4	1722	Ketones	-	+	Unwashed
			-	+	Washed
5	1725	Terminal methyl ketones	-	+	Unwashed
			-	+	Washed
6	1737	Esters and aldehyde	-	+	Unwashed
			-	+	Washed
7	1739	Esters	+	-	Unwashed
			+	-	Washed
8	1743	Esters and peresters	+	-	Unwashed
			+	-	Washed
9	1750	Peracids	+	-	Unwashed
			+	-	Washed
10	1756	Free carboxylic acids	+	-	Unwashed
			+	-	Washed
11	1767	Carboxylic acids (isolated)	-	+	Unwashed
			-	+	Washed
12	1784	$\gamma$ -Lactones	-	+	Unwashed
			-	+	Washed
13	1791	Not identified	-	+	Unwashed
			-	+	Washed

our group have also observed a similar time dependence of some carboxylic groups' accumulation.<sup>5,6</sup> Indeed, in protocols carried out in the city of Laghouat in Algeria on the same type of samples, Yagoubi et al. and our group showed the same qualitative species with predominance of aldehydes but with a converse concentration of ketones and carboxylic acids.<sup>6</sup>

In the present study it was found that the kinetic formation of the carbonyl species was somewhat different when the films were washed than when they were unwashed. In both cases the aldehydes were the predominant species with a higher concentration, by about 10%, for the washed film after 6 months than for the unwashed ones. However, even though the difference in final concentration was not very large the evolution was indeed very different. For the unwashed ones the aldehydes increased slowly during the first 2 months, followed by a constant concentration during 2 months and then it became autoaccelerated. However, for the washed ones, their increase was progressive. Another fact not negligible is the formation of ketones was different since they developed more for the unwashed ones.

**Table 2.** Concentrations of aldehydes, carboxylic acids, ketoacids, ketones,  $\gamma$ -lactones, and esters in naturally weathered UU and UW 2100 T N00W films.

Concentration (mmol/L)	Aging (months)							Washing
	0	1	2	3	4	5	6	
<b>Aldehydes</b>	0.22	11.14	16.11	16.53	17.83	23.96	50.88	U
	0.07	15.53	23.90	33.24	40.99	50.97	61.23	W
<b>Acids</b>	0	2.53	9.87	11.50	12.24	13.32	19.28	U
	0	1.92	4.67	12.64	15.88	18.19	22.83	W
<b>Ketoacids</b>	0	0	1.80	6.74	8.65	7.82	12.78	U
	0	0	4.01	0.57	3.44	10.30	11.90	W
<b>Ketones</b>	0	2.14	9.73	10.36	9.87	9.76	14.34	U
	0	1.80	3.29	4.67	5.08	5.57	6.04	W
<b><math>\gamma</math>-Lactones</b>	0	0.72	1.41	2.42	2.99	3.59	3.70	U
	0	0.70	1.68	2.95	2.39	2.99	4.67	W
<b>Esters</b>	0.39	0.24	0.73	0.46	1.02	1.45	2.45	U
	0.40	0.27	0.55	0.79	0.83	1.31	2.01	W

The results shown in Table 2 mean that washing accelerated and increased the formation of aldehydes ( $1733\text{ cm}^{-1}$ ), known to be supplied by the decomposition of hydroperoxides.<sup>3</sup> The graphical representation of the hydroperoxide index (HI) as a function of aldehydes concentration shows well that there existed an almost linear relationship between these two species when the films were washed (Figure 6). In fact, the correlation coefficient was about 0.98, indicating a close linear relationship between these two species. However, for the unwashed films the progression looks like an s-shaped curve, showing that the hydroperoxides did not contribute to aldehyde formation in the period included between 2 and 4 months, followed by a vertical increase in hydroperoxides. After this time limit, the aldehyde formation restarted, further increasing hydroperoxide production. Therefore, both curves highlight the chemical relationship existing between hydroperoxide consumption and aldehyde formation.

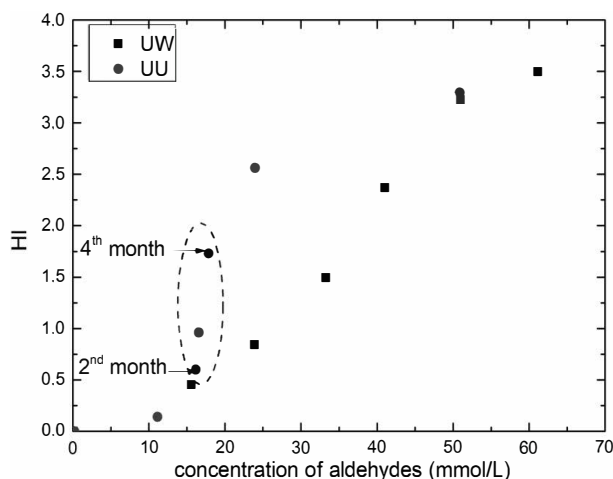
**Figure 6.** Hydroperoxide index (HI) as function of aldehyde concentration.

Table 2 and the curve shape of Figure 6 suggest that not washing prevents oxidation during the middle period of the aging protocol due to thin-layer formation of dust and degraded material, besides the low sunshine in this period. For longer periods of exposure, this protective layer became inefficient since it seems that beyond a limit of time it cannot protect the film anymore from the deleterious effect of irradiations.

The carbonyl and hydroperoxide indexes versus exposure time of unstabilized and stabilized samples are reported in Table 3, respectively. As expected, the stabilized samples presented negligible CI and HI variations until the end of exposure. However, the HI of the unwashed stabilized films was slightly higher and followed the same variations as for the washed ones. For the unstabilized films, the CI and HI were much higher and give a good insight into the occurrence of significant microstructural changes, with the washed samples having slightly higher indexes than the unwashed ones. Washing significantly increased the CI slope and the end value was 11 against 6 for the unwashed ones. It is thought that polyethylene films enter the decay stage when CI is greater than 6 and enter the embrittlement stage for CI greater than 45.<sup>23,24</sup> Therefore, the washed samples (UW) started decaying within only 3 months of exposure while the unwashed (UU) ones decayed after 6 months and none of the films were embrittled.

**Table 3.** Carbonyl index (CI), hydroperoxide index (HI), and vinyl index (VI) of UU, UW, SU, and SW LDPE films.

CI						HI					
Aging (months)	Sample		Aging (months)	Sample		Aging (months)	Sample		Aging (months)	Sample	
	UU	UW		SU	SW		UU	UW		SU	SW
0	0	0	0	0	0	0	0	0	0	0	0
1	2.1	2.23	2	0.26	0.25	1	0.14	0.44	2	0.39	0.21
2	2.9	5.55	4	0.35	0.34	2	0.59	0.83	4	0.61	0.23
3	3.2	6.22	7	0.47	0.38	3	0.96	1.48	7	0.59	0.26
4	4.6	8.30	10	0.44	0.56	4	1.73	2.37	10	0.41	0.04
5	4.8	10.52	13	0.54	0.37	5	2.56	3.27	13	0.21	0.03
6	6.8	11.38	16	0.76	0.38	6	3.29	3.52	16	0.07	0.01
			19	0.50	0.28				19	0.31	0.03
VI											
Aging (months)	Sample		Aging (months)	Sample							
	UU	UW		SU	SW						
0	0	0	0	0	0						
1	0.1	0.1	2	0.07	0.07						
2	0.18	0.19	4	0.07	0.08						
3	0.18	0.20	7	0.08	0.09						
4	0.20	0.22	10	0.09	0.1						
5	0.22	0.27	13	0.1	0.1						
6	0.33	0.35	16	0.11	0.11						
			19	0.12	0.12						

The formation of vinyls ( $909\text{ cm}^{-1}$ ) (Figure 5a) increased drastically for each of the washed and unwashed unstabilized films (Table 3) during the entire duration of the aging protocol. For the stabilized ones, despite a longer exposure period, the growth of VI was less pronounced than for the unstabilized grade during the same 6 months of exposure and then the VI nearly plateaued as seen in the table; washing had essentially a negligible effect for both types of film.

In an attempt to highlight any difference between the two types of film, curve fitting of the  $910\text{ cm}^{-1}$  band was done but did not reveal the existence of hidden absorption bands other than the principal absorption. The same treatment, when done on the resonance vibration of the vinyl species at  $1640\text{ cm}^{-1}$ , revealed a clear difference between the two types of film (Figures S2 and S3). For the unstabilized unexposed films (Figure S2a),



curve fitting revealed three different peaks at 1635, 1640, and 1645  $\text{cm}^{-1}$ , attributed to trans-vinylene for the first and vinyls for the second and third (Table 4). At the end of exposure (Figure S2b), the absorption band intensity increased drastically and the three subpeaks “fused” to give only one intensive band peaking at 1640  $\text{cm}^{-1}$ ; the areas and the intensity of the respective peaks were compared by a superposition and were found to be the same for each of them (unwashed and washed).

**Table 4.** Assignment of the component bands in the vinyl region.

Component	Peak positions ( $\text{cm}^{-1}$ )	Assignment	Washing	Unstabilized LDPE		Stabilized LDPE	
				Aging (months)			
				0	6	0	19
1	1609	Not identified	U	-	-	+	-
			W	-	-	-	-
2	1615	Vinyl ketones	U	-	-	+	1618
			W	-	-	+	1618
3	1624	Vinyl ketones	U	-	-	+	1625
			W	-	-	+	1629
4	1635	Trans-vinylene	U	+	-	+	1631
			W	+	-	+	+
5	1640	Vinyls	U	+	+	+	1637
			W	+	+	+	1641
6	1645	Vinyls	U	+	-	+	1643
			W	+	-	+	+

For unexposed, stabilized samples (Figure S3a), curve fitting revealed the presence of more subpeaks (six) with the main and most intensive one peaking at 1624  $\text{cm}^{-1}$ . The wavenumber range was also wider, extending from 1600 to 1650  $\text{cm}^{-1}$ . After 19 months of exposure, the number of subpeaks dropped to five and the absorption band shifted from 1600 to 1610  $\text{cm}^{-1}$  on its right side (Figures S3b and S3c; Table 3). It was also noted that the intensity of the absorption band was globally lowered. A comparison between the spectra of the two aged sample types showed well that washing affected the intensity (Figures S3b and S3c) and the peak position of the subpeaks (Table 4).

### 2.3. Crystallinity index

The crystallinity degrees obtained by DSC for both unstabilized and stabilized polyethylene films are listed in Table 5. The crystallinity of the unstabilized film was higher than that of the stabilized one. It was about 35% for the U0 and 30% for the S0 grade. The crystallinity degree increased to 49% and 43% for UU6 and SU19, the last aging stage of the respective grades. However, washing lowered the rate of crystallinity increase, which became only 47% and 42% for UW6 and SW19, respectively. The lowering of crystallinity can be explained by the fact that washing removed the layer of dust and highly degraded and detached elements of the material surface. This also includes the deteriorated additives having migrated due to physical and chemical processes associated with the stabilizer (UVA, HALS).<sup>25</sup>

The crystallinity determined by ATR showed not only the expected increase in crystallinity with aging

**Table 5.** Crystallinity of unwashed and washed unstabilized and stabilized LDPE films before and after natural weathering.

Crystallinity degree (%)	Washing	Unstabilized LDPE		Stabilized LDPE	
		Aging (months)			
		0	6	0	19
DSC	U	35	49	30	43
	W		47		42
ATR	U	55	67	57	65
	W		61		60

but also higher values compared to those obtained by DSC (Table 5). The crystallinity degree increased by 22% and 14% for UU6 and SU19, respectively, but it was only the half (11%) for UW6 and even lower (5%) for SW19. The difference between the two techniques was due to the fact that DSC is based on the melting of the entire material volume, while ATR measures only inside a thin layer of the film surface. The relevant values obtained by ATR for washed samples confirm the idea that washing eliminated the highly degraded material building up on the surface. This also gives a good insight into the crystallinity and the oxidation profile with a decreasing value and concentration, respectively, toward the core of the film. The microstructural changes undergone by the material (chains oxidation) led to the increase in crystallinity.

In general, the loss of mechanical properties with increasing aging time is highly related to the increase in the crystallinity degree and then the decrease in the molecular weight.<sup>16</sup> One of the remaining questions was does washing affect the mechanical properties? That is dealt with in the next section.

#### 2.4. Tensile tests

Figure 7 shows the stress–strain curves of UU, UW, SU, and SW samples for different aging stages. For the unaged samples (Figures 7a–7d) after an initial linear deformation the slope of the curve changed, attesting yield occurring. The deformation was characterized then by a necking. The samples then underwent a short cold drawing followed by a progressive increase in the amount of strain to display finally a significant degree of strain hardening indicated by a large positive slope. The extension ultimately ended in a ductile rupture of the material.

For the UU samples (Figure 7a), the curves shape changed progressively with aging, characterized by a slight lowering of the yield stress and stress at break. The slope of the strain hardening and its portion of the curve diminished until it vanished and the material displayed only the cold drawing portion, which became a little longer. The same types of effects were observable for the stabilized type (Figures 7c and 7d). However, washing affected the tensile behavior of the material (Figures 7b and 7d). The best way to highlight the effect of washing is to describe its effect on the different mechanical parameters, namely Young's modulus ( $E$ ), and the failure stress ( $\varepsilon_b$ ) and strain ( $\sigma_b$ ), reported in Figures 8–10. In Figures 8a and 8b are displayed Young's modulus of the two types of samples. For the two unaged films the modulus was almost the same (173 MPa for unstabilized and 169 MPa for stabilized). During the whole period of exposure, Young's moduli increased and remained greater for the unstabilized films, except for SU 13, and, moreover, were higher for the washed samples (251 and 228 MPa for UW and SW against 229 and 204 MPa for UU and SU) after 6 and 19 months than for the unwashed ones.

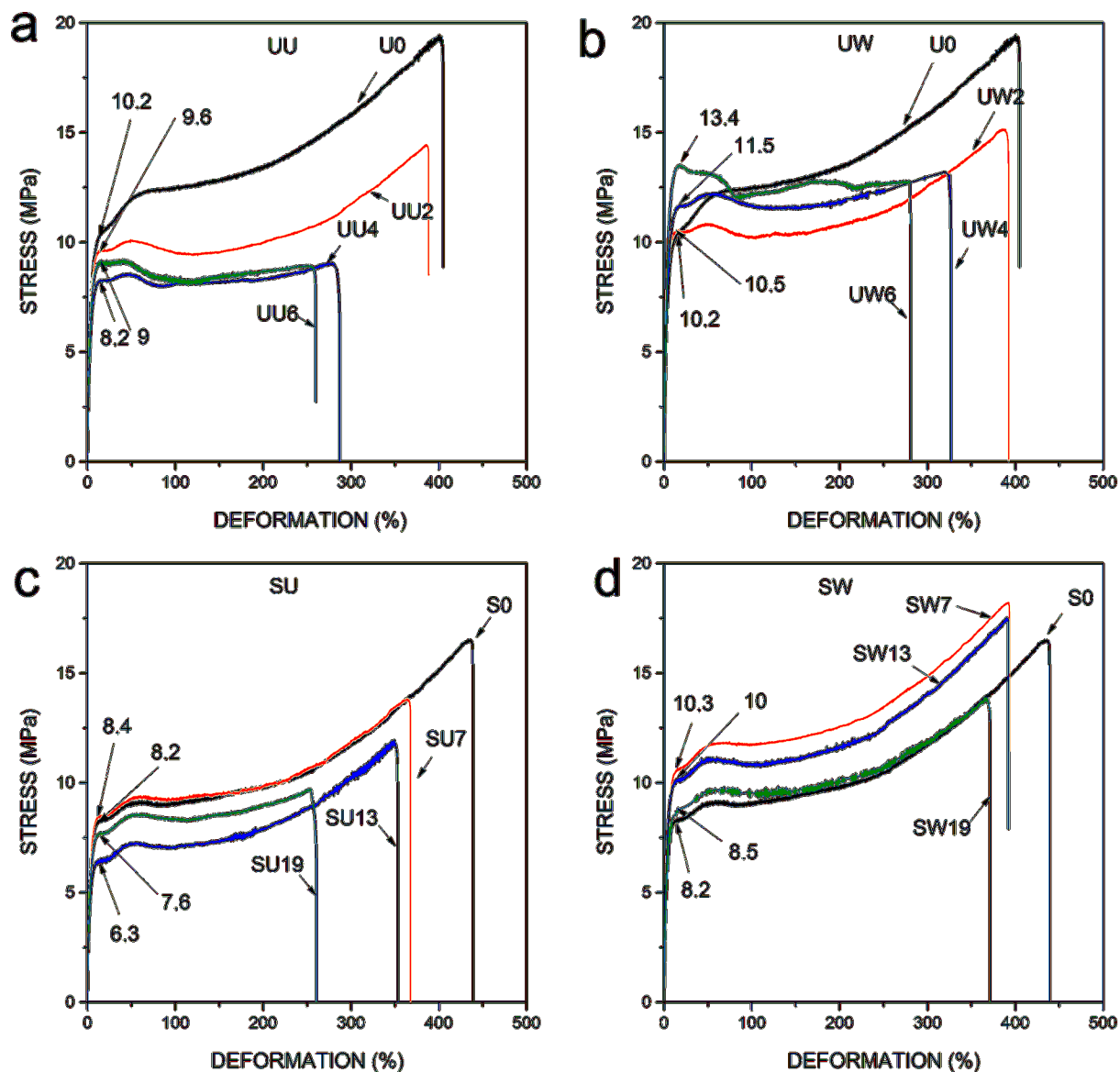


Figure 7. Stress–strain curves for naturally weathered UU (a), UW (b), SU (c), and SW (d) LDPE 2100T films.

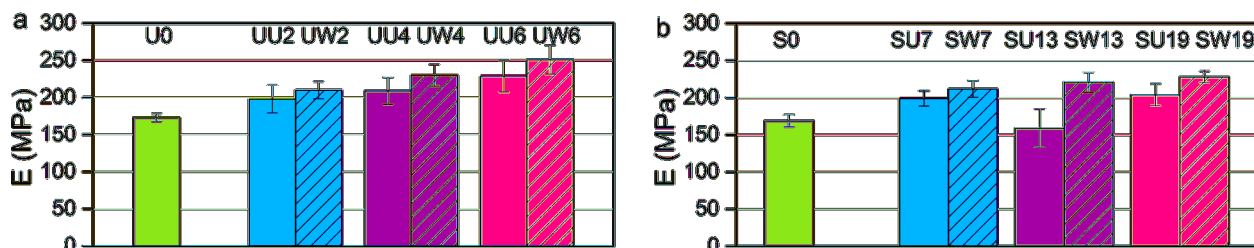


Figure 8. Variation in Young's modulus with exposure time: a) unstabilized, b) stabilized LDPE 2100T films.

The variations in the failure stress and strain ( $\sigma_b$ ,  $\varepsilon_b$ ) as a function of exposure time are represented in Figures 9 and 10, respectively. The stress at failure ( $\sigma_b$ ) displayed a different behavior for the two types of

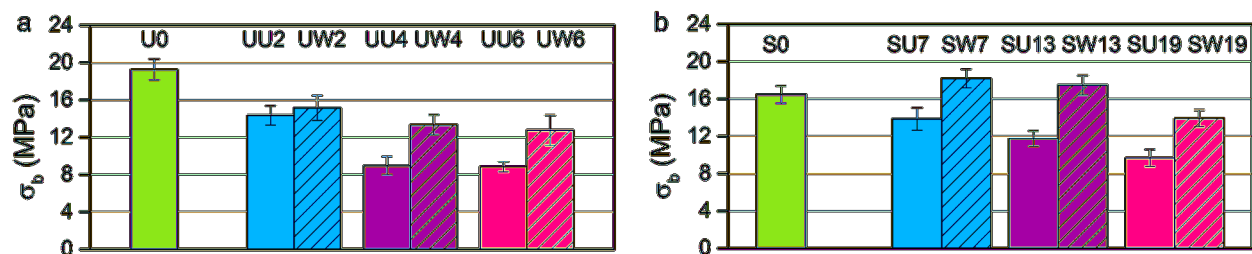


Figure 9. Variation in failure stress with exposure time: a) unstabilized, b) stabilized LDPE 2100T films.

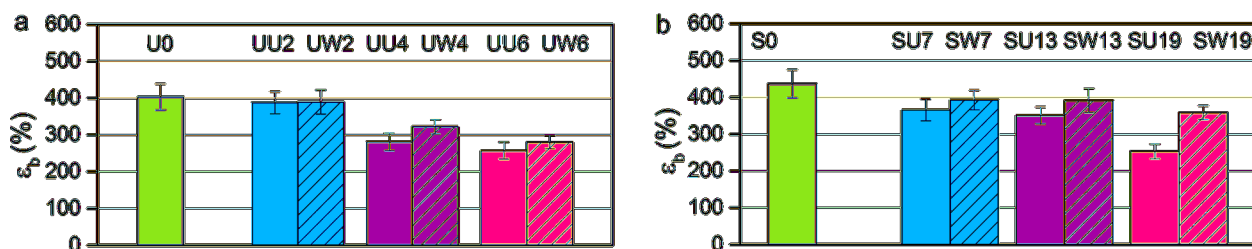


Figure 10. Variation in failure strain with exposure time: a) unstabilized, b) stabilized LDPE 2100T films.

film. The unaged, unstabilized sample (Figure 9a) had a higher value by almost 20% compared to the unaged stabilized one (Figure 9b). However, for the unwashed samples  $\sigma_b$  decreased more and more quickly with aging for the unstabilized type, since at the last aging stage  $\sigma_b$  of the SU was higher by about 11% after 19 months of exposure, compared to the UU sample exposed for only 6 months.

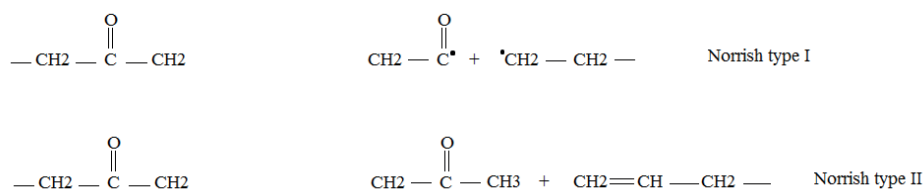
For the stabilized type, the failure stress behavior was different between washing and not washing; the SW samples displayed a slight reinforcement of this property until 7 months and then started to slightly decrease at 13 months and this became more intensive at 19 months. However, for the SU samples it dropped more drastically, without any reinforcement at short times. The overall results showed that the variation in this property decreased much more slowly with washing. Indeed, their respective degrees of decrease were 34% and 15% for UW and SW and 54% and 41% for UU and SU.

The failure strain ( $\varepsilon_b$ ) for the U0 film (Figure 10a) was slightly lower than that of the S0 film (Figure 10b). For both types the elongation at break decreased progressively with aging. The decreasing variation in this property was more important for the UU samples than for the SU ones; this is because the latter life time was longer. Washing tended to lower the rate of decrease, with decreases of 31% (UW6) and 18% (SW19) against 36% (UU6) and 42% (SU19).

The overall results showed that natural weathering led to an irremediable molecular structure alteration of the films' surface that progressed in the direction of the core. This mainly led to microstructural modifications (chain oxidation, section 2.2) followed by a crystallinity increase (section 2.3), which had a direct impact on the mechanical properties (section 2.4). The addition of stabilizers tended to lower the stiffness of both the unaged and aged films but reinforced the failure stress ( $\sigma_b$ ) during a relatively long period and remarkably delayed its drop when exposed. Aging is the occurrence of competition between crosslinking and chain scission reactions, with the crosslinking tending to reinforce the mechanical properties while the chain scissions lower them.<sup>16</sup>

Indeed, the decreasing variation in the failure strain ( $\varepsilon_b$ ) observed for the two types of LDPE film with aging indicated that the embrittlement of the material occurred more slowly and with a lower amount of failure

strain. The decrease in failure strain is explained by the occurrence of chain scissions resulting from Norrish type I and II reactions. However, washing had a significant influence on the failure strain. For unstabilized samples, it delayed the decrease in failure strain but less than for stabilized samples due to the presence of stabilizers in them (stabilized films). In their study on HALS stabilization of LDPE films used in agricultural applications, Kaci et al. found that HALS stabilizers prevented the occurrence of Norrish type I and II reactions, delaying the decrease in the material failure strain as a result.<sup>25</sup>



However, the presence of stabilizers in addition to washing delayed the failure strain more. After 19 months of exposure, the loss was about 46% for the unwashed sample compared to its initial value, while for the washed one it was only 18%. This means that the washing process reinforced this property ( $\varepsilon_b$ ), extending the lifetime of the material. In fact, the washing process removed the highly degraded particles attached to the film surface (constituted by amorphous chain segments and crystalline parts), reducing slightly the crystallinity degree measured by both DSC and ATR at the end of the aging process for both types of film. However, the higher crystallinity degree values found by ATR compared to DSC can be explained by the fact that ATR is a surface measurement while DSC is volume based. The removal of the thin layer of degraded material revealed a new virgin surface allowing deeper penetration of the sun irradiation in the direction of the material core. Consequently, the oxidation was more significant and, unexpectedly, it appears that it contributed to improve the ultimate mechanical properties.

In conclusion, LDPE films for greenhouse covering were naturally weathered in a sub-Saharan facility (Ghardaïa, Algeria). Besides natural weathering, the effect of washing on the film properties was checked by various techniques. The quantitative estimation of the carbonyl species analyzed by FTIR revealed that washing enhanced their final concentrations. However, it did not qualitatively affect the carbonyl species formation as verified by curve fitting.

Washing promoted a linear relationship between hydroperoxide index and aldehyde formation provided by the decomposition of the former, explained by the removal of an existing thin layer of highly degraded material that tended to temporarily protect the material from degradation. Indeed, for unwashed samples, this thin layer inhibited hydroperoxide decomposition for several months but not for the total duration of exposure. Washing led to lower increases in crystallinity indexes with aging, improving consequently the ultimate mechanical properties of the material.

To summarize, it can be said that washing removed the dust and the thin layer of degraded material, revealing a new virgin surface ready for irradiation absorption. This is why washed samples were more oxidized; however, against all expectations, the ultimate mechanical properties were found to be better than those of the unwashed film, meaning that washing delayed the loss of mechanical properties.

### 3. Experimental

#### 3.1. Material

The commercial samples (one stabilized (S) and the other unstabilized (U)) were supplied by Saudi Basic Industries Corp (SABIC) as "LDPE 2100 T N00W" (their density and melt flow index (MFI) were 0.92 g/cm<sup>3</sup>

and 0.33 g/10 min). The films were produced by blowing extrusion at Sofiplast, an Algerian company located at Sétif. The drawing speed of the production line was fixed to 15 cm/s. The melt was extruded at about 175 °C and blown in a continuous process characterized by a bubble diameter of 4.4 m and a wall thickness of 160 µm. The expansion ratio and die opening were not available.

The stabilizing additives represented 6% of the film weight. It was made of mineral charges (kaolin), ultraviolet absorbers (UVAs), hindered amine light stabilizer (HALS) (with a dosage of 7%–10% according to the film thickness assuring 7000 ppm to 10,000 ppm), and heavy metals, which gave a pistachio color to the film.

### 3.2. Exposure

The exposure took place in Ghardaïa, Algeria (32°29'N, 3°40'E), for a total duration of 6 months for the unstabilized grade (U) and 19 months for the stabilized one (S), starting from October 2012. The films were exposed on a south-oriented metal support, inclined by 32° with respect to the horizontal, according to the NF51-165 standard. Sampling was done bimonthly for the unstabilized grade and every 3 months for the stabilized one, from the film zones distant from the contact points with the holding frame. This precaution was taken to avoid an uncontrolled overheating of the material. The washing was done by spraying once a day with cold water (ambient temperature  $\approx 18$  °C). The washed samples are labeled “W” to distinguish them from the unwashed ones “U”, i.e. (SU: stabilized unwashed, SW: stabilized washed, UU: unstabilized unwashed, UW: unstabilized washed). It needs to be pointed out that the data presented for the unexposed films are for only one type of film per grade since the unexposed material did not undergo a washing process.

### 3.3. Solar energy

The incident solar energy was measured by an electrical assembly consisting of a solar cell and a galvanometer, placed at the same angle and in parallel to the metal panel (Figure 11). The recorded values were then converted to energy using Eqs. (1) and (2), where  $I$  is the solar current intensity.

$$E = \begin{cases} 18665.24 \times I - 110.18717 & \text{for } I < 20 \text{ mA} \\ 1626.51 \times I + 208.47974 & \text{for } I > 20 \text{ mA} \end{cases} \quad (1)$$

(2)

### 3.4. IR spectroscopy

FTIR spectroscopy analysis was conducted on a Spectrum Two unit (PerkinElmer, Inc., USA). It provided information on the functional groups present in the samples for the wavelength range from 4000 to 400  $\text{cm}^{-1}$ . Scans were run at a resolution of 4  $\text{cm}^{-1}$  in transmission.

The presence of isolated and associated (H-bonded) hydroperoxides was monitored at 3552  $\text{cm}^{-1}$  and 3410  $\text{cm}^{-1}$ , respectively. The hydroperoxide index (HI) is defined as the ratio of the integrated area (IA) of the absorption bands at 3552  $\text{cm}^{-1}$  and 2010  $\text{cm}^{-1}$  ( $\text{HI} = \text{IA}_{3552} / \text{IA}_{2010}$ ). The band centered at 2010  $\text{cm}^{-1}$ , due to its being unchanged, was used as the reference band.<sup>5</sup> In order to enhance the sensitivity, the integrated absorbance peaking at 3600  $\text{cm}^{-1}$  band was measured after subtraction of the spectrum of the corresponding initial sample. In a similar way, the overall variety of carbonyl species present in the wide carbonyl absorption band was included in the carbonyl index (CI), which is defined as the integrated area (IA) of the whole 1800–1650  $\text{cm}^{-1}$  carbonyl band divided by the IA of the 2010  $\text{cm}^{-1}$  band;  $\text{CI} = \text{IA}_{1800-1650} / \text{IA}_{2010}$ . The vinyl



**Figure 11.** Solar cells (right) for the energy measurement during natural weathering.

index (VI) is defined as the ratio of the IA of the band at  $909\text{ cm}^{-1}$  divided by the integrated intensity of the  $2010\text{ cm}^{-1}$  band.

The ATR spectra, used for calculating the crystallinities, were obtained by analyzing the films' surface in contact with a crystal diamond. The crystallinities of the LDPE films were determined using the method described by Zerbi et al.:<sup>26,27</sup>

$$X (\%) = \left( 1 - \left( \frac{I_b - I_a}{1.233 (I_b + I_a)} \right) \right) \times 100 \quad (3)$$

where  $I_a$  and  $I_b$  are the peak areas of the characteristic ATR bands intensity at  $1474$  and  $1464\text{ cm}^{-1}$ , corresponding to the bending deformations of the methylene ( $\text{CH}_2$ ) groups in the crystalline ( $1474\text{ cm}^{-1}$ ) and amorphous ( $1464\text{ cm}^{-1}$ ) phases, respectively. The constant 1.233 is the relation between these two ( $1474\text{ cm}^{-1}$  and  $1464\text{ cm}^{-1}$ ) areas for a completely crystalline polyethylene.<sup>28,29</sup>

Curve-fitting analysis of the carbonyl and vinyl curves was performed with the OriginPro software package (Version 9.0). The normalized IR spectra of the samples were processed in the  $1800\text{--}1680\text{ cm}^{-1}$  carbonyl region. The Gaussian distribution and baseline subtraction were used as the deconvolution strategy. The Gaussian profile provides the best fit<sup>30</sup> and was theoretically verified by the Doppler effect.<sup>31</sup> The quality of the fit was checked using the determination coefficient, which was  $R^2 > 0.9998$  for the absorption band of each sample. The residual sum of the squares was determined to be chi-squared  $< 10^{-5}$ .

According to the Lambert–Beer equation, the concentration  $C$  ( $\text{mol L}^{-1}$ ) of an analyte is given by

$$C = \frac{IA}{\varepsilon \times b} \quad (4)$$

where IA ( $\text{cm}^{-1}$ ) is the integrated intensity (area) of a characteristic IR absorption band of the analyte, b (cm) is the sample thickness and  $\varepsilon$  ( $\text{cm mmol}^{-1}$ ) is the integrated extinction coefficient, a proportionality factor peculiar to the absorption band. The amount of the different carbonyl species could be estimated directly from the integrated absorbance areas of the respective components resolved by curve fitting, provided that their extinction coefficients were known. Unfortunately, to the best of the authors' knowledge, the extinction coefficients of only a few of the carbonyl species are available in the literature.<sup>32,33</sup> Details of the calculation methods for the different species' contributions (aldehydes, carboxylic acids, ketoacids, ketones, lactones, and esters) were described by Salvalaggio et al.<sup>5</sup>

### 3.5. Tensile tests

The stress–strain curves for all of the samples were obtained using a tensile machine (Zwick/Roell Group, USA) at room temperature ( $T = 21 \pm 1^\circ\text{C}$ ) at a nearly constant relative humidity ( $\text{RH} = 50 \pm 5\%$ ). The rectangular tensile test specimens were cut out of the original and the aged films, for the two grades (U and S) and the unwashed and washed ones, with an overall length of  $L_0 = 70$  mm, gauge length  $L_G = 50$  mm, width  $W_0 = 10$  mm, and thickness  $T_0 = 0.16$  mm. The strain rate was set at  $d\varepsilon/dt = 3.33 \text{ s}^{-1}$  to characterize both Young's moduli and the properties at failure.

### Acknowledgment

The authors would like to thank Dr Bouhadda Youcef (Applied Research Unit in Renewable Energies (ARURE/CDER) Ghardaïa, Algeria) for his assistance during part of this study.

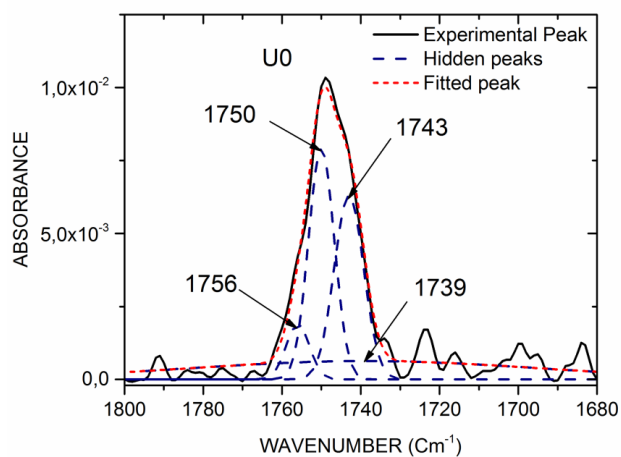
### References

1. Reich, L.; Stivala, S. S. *Autoxidation of Hydrocarbons and Polyolefins*. Marcel Dekker: New York, NY, USA, 1969.
2. Iring, M.; Tüddös, F. *Prog. Polym. Sci.* **1990**, *15*, 217-262.
3. Tidjani, A. *Polym. Degrad. Stab.* **2000**, *68*, 465-469.
4. Chabira, S. F.; Sebaa, M.; G'sell, C. *J. Appl. Polym. Sci.* **2008**, *110*, 2516-2524.
5. Salvalaggio, M.; Bagatin, R.; Fornaroli, M.; Fanutti, S.; Palmery, S.; Battistel, E. *Polym. Degrad. Stab.* **2006**, *91*, 2775-2785.
6. Yagoubi, W.; Abdelhafidi, A.; Sebaa, M.; Chabira, S. F. *Polym. Test.* **2015**, *44*, 37-48.
7. Benmiloud, N. H.; Sebaa, M.; Chabira, S. F.; Ponçot, M.; Royaud, I.; *J. Appl. Polym. Sci.* **2016**, *133*, 1-8.
8. White, J. R.; Turnbull, A. *J. Mater. Sci.* **1994**, *29*, 584-613.
9. Khan, J. H.; Hamid, S. H. *Polym. Deg. Stab.* **1995**, *48*, 137-142.
10. Sebaa, M.; Servens, C.; Poyet, J. *J. Appl. Polym. Sci.* **1993**, *47*, 1897-1903.
11. Fechinea, G. J. M.; Rabellob, M. S.; Souto-Maiora, R. M. *Polym. Deg. Stab.* **2002**, *75*, 153-159.
12. George, S. *Infrared and Raman Characteristic Group Frequencies, Tables and Charts*; Wiley: Chichester, UK, 2001.
13. Yucheng, F. U.; Loong-Tak, L. *Polym. Test.* **2012**, *31*, 56-67.
14. Feuillolery, P.; César, G.; Benguigui, L.; Grohens, Y.; Pillin, I.; Bewa, H.; Lefaux, S.; Jamal, M. *Polym. Enviro.* **2005**, *13*, 349-355.
15. Boulos, Y.; Dehbi, A.; Hamou, A.; Saiter, J. M. *Mater. Des.* **2008**, *29*, 2017-2020.
16. Chabira, S. F.; Sebaa, M.; Huchon, R.; De Jeso, B. *J. Polym. Degrad. Stab.* **2006**, *91*, 1887-1895.
17. Costa, L.; Luda, M. P.; Trossareilli, L. *Polym. Degrad. Stab.* **1997**, *58*, 41-54.

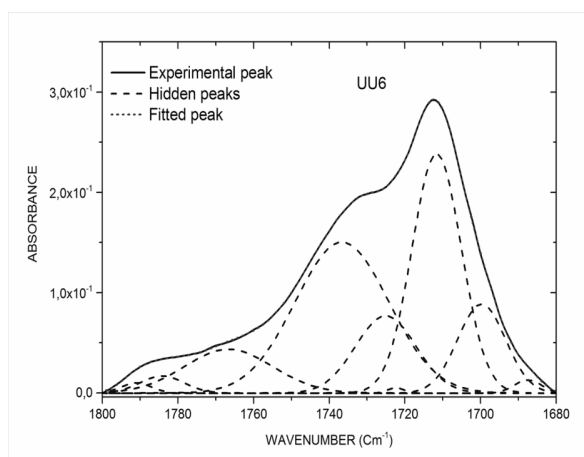


18. Teissedre, G.; Pilichowski, J. F.; Chmela, S.; Lacoste, J. *Polym. Degrad. Stab.* **1996**, *53*, 207-215.
19. Zweifel, H.; Maier, R. D.; Schiller, M. *Plastics Additives Handbook*. 6th Ed; Carl Hanser Verlag: Munich, Germany, 2009.
20. Gulmine, J. V.; Janissek, P. R.; Heise, H. M.; Akcelrud, L. *Polym. Degrad. Stab.* **2003**, *79*, 385-397.
21. Yang, R.; Christensen, P. A.; Egerton, T. A.; White, J. R. *Polym. Degrad. Stab.* **2010**, *95*, 533-541.
22. Barcelo, D. In *Molecular Characterization and Analysis of Polymers*; Chalmers, J. M.; Meier, R. J., Eds.; Elsevier: New York, NY, USA, 2008, pp. 387.
23. Roy, P. K.; Surekha, P.; Rajagopal, C.; Chatterjee, S. N.; Choudhary, V. *Polym. Degrad. Stab.* **2007**, *92*, 1151-1160.
24. Lin, Y. *Appl. Polym. Sci.* **1997**, *63*, 811-818.
25. Kaci, M.; Sadoun, T.; Cimmino, S. *Macromol. Mater. Eng.* **2000**, *278*, 36-42.
26. Zerbi, G.; Gallino, G.; Del Fanti, N.; Baini, L. *Polymer* **1989**, *30*, 2324-2327.
27. Guo, J. J.; Yan, H.; Bao, H. B.; Wang, X. M.; Hu, Z. D.; Yang, J. J. *Spectrosc. Spect. Anal.* **2015**, *35*, 1520-1524.
28. Lin, L.; Argon, A. S. *Mater. Sci.* **1994**, *29*, 294-323.
29. Meijer, H. E. H.; Govaert, L. E. *Prog. Polym. Sci.* **2005**, *30*, 915-938.
30. De Aragão, B. J. G.; Messaddeq, Y. *J. Braz. Chem. Soc.* **2008**, *19*, 1582-1594.
31. Bernath, P. F. *Spectra of Atoms and Molecules*. 2nd ed.; Oxford University Press: Oxford, UK, 2005.
32. Rugg, F. M.; Smith, J. J.; Bacon, R. C. *J. Polym. Sci.* **1954**, *13*, 535-547.
33. Fodor, Z. S.; Iring, M.; Tüdös, F.; Kelen, T. *J. Polym. Sci. Polym. Chem.* **1984**, *22*, 2539-2550.

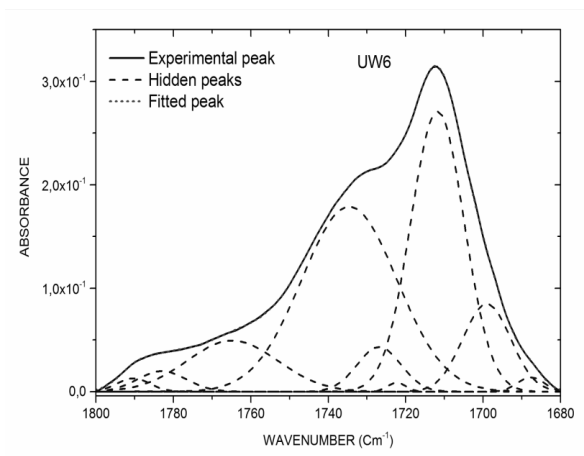
## Supplementary material



(a)



(b)



(c)

**Figure S1.** Deconvolution analysis of the IR carbonyl band of unstabilized LDPE film unaged (a) and weathered for 6 months; unwashed (b), washed (c).

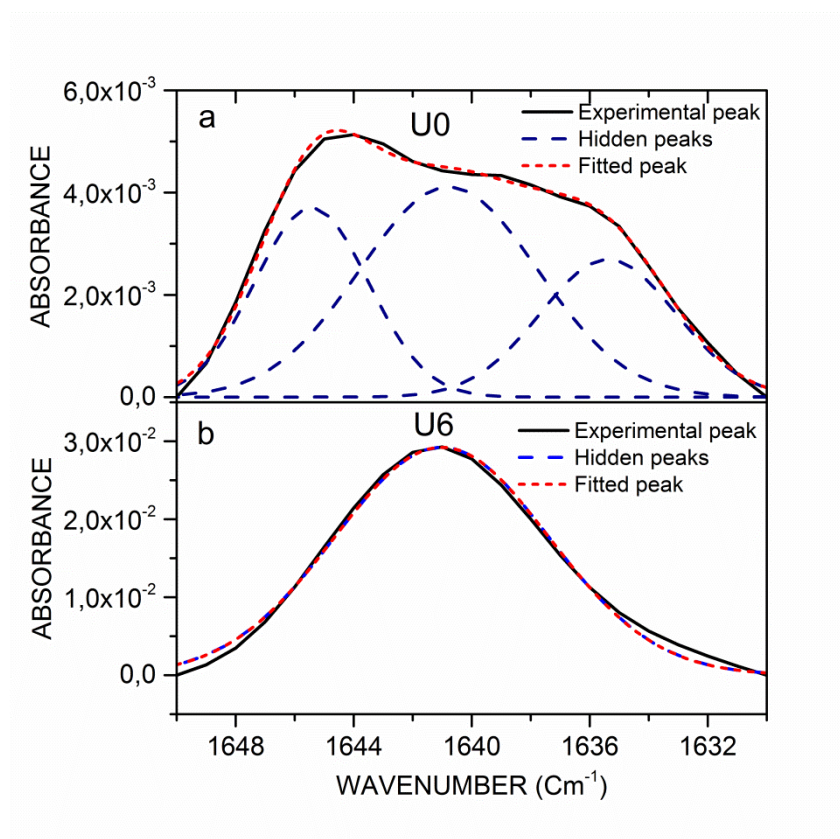
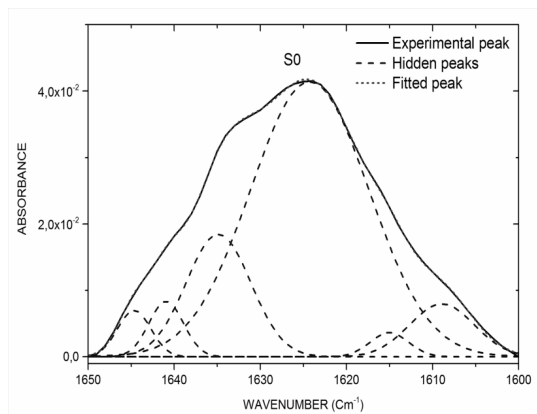
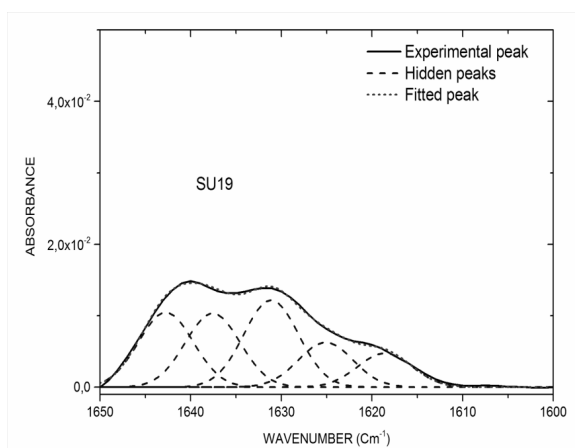


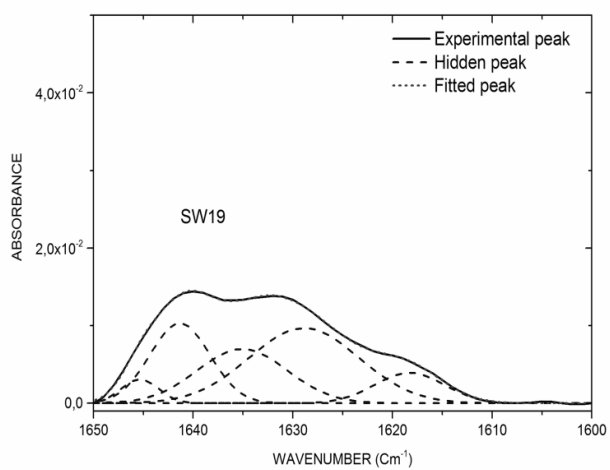
**Figure S2.** Deconvolution analysis of the IR vinyl absorption of unstabilized unwashed LDPE films before (a) and after (b) 6 months of exposure. The curves were identical for the washed samples.



(a)



(b)



(c)

**Figure S3.** Deconvolution analysis of the IR vinyl absorption of stabilized LDPE films before (a) and after (b, c) 19 months of exposure; b) unwashed samples, c) washed samples.